Modelling the Fate of Dredged Material Following Disposal at the Nab Tower Disposal Site

Author(s): David M. Kelly, Liam Fernand, Jon Rees, Stefan Bolam.

Date in format: November 2021

www.cefas.co.uk

Cefas Document Control

Submitted to:	The Marine Management Organisation
Date submitted:	22nd November 2021
Project Manager:	Andrew Soanes
Report compiled by:	David Kelly
Quality control by:	John Bacon
Approved by and date:	Andrew Soanes 22nd November 2021
Version:	V2.0
Recommended citation for this report:	

Modelling Quality control checklist			
	Originator	Check	Comments
Source data, e.g. bathymetry, rivers etc.	Kelly	Fernand	Details given, suitable for this purpose
Validation	Kelly	Fernand	Tidal: Very good for both tidal currents and water levels
Calibration	Kelly	Fernand	Flow calibrated against ADCP data for depth-averaged current components

Run Scenarios	Kelly	Fernand	3D runs defined with through discussion with LF, JR and SB.

Version control history

Version	Author	Date	Comment
v.0.1	Kelly	10th March 2021	Initial draft for internal review
v0.2	Kelly, Fernand, Bolam	16th March 2021	
v0.3	John Bacon	22nd March 2021	QA version
v0.4	Stefan Bolam	26th March 2021	QC version
v0.5	Andrew Soanes	30th March 2021	Review
v1.0	Andrew Soanes	30th March 2021	Submission
v2.0	Andrew Soanes	22nd November 2021	Final version

Executive Summary

The purpose of this report is to detail the 3D modelling of the fate of dredged material at the Nab Tower (NT) disposal site and to present the modelling outcomes with respect to the fate of dredged material disposed at the site. Specifically, the report focuses principally on the likelihood of the placed material being subsequently relocated to, and being deposited on, the seabed within the Bembridge MCZ which was designated in May 2019. The outcomes will, therefore, be of utility for the MMO in responding to any concerns whether disposal activity may be responsible for benthic smothering impacts within the MCZ or elsewhere in the region.

The Nab Tower disposal site is located approximately 8 -13 km south east of the Isle of Wight (Figure 1). The disposal site is approximately 5.5 km by 2.3 km in size. Water depths at the site and in its vicinity range from 20 m to 40 m; in such water depths in this part of the Eastern English Channel, the dispersal of dredged material, as well as deposition and erosion, is primarily driven by tidal currents. Additionally, depending on wind severity, a proportion of sediment dispersal may be driven by wind induced currents. The purpose of the modelling undertaken here is to replicate these processes. As such, it is important to correctly reproduce the ambient hydrodynamic conditions as they will be responsible for sediment advection and resuspension processes and, hence, sediment dispersion patterns. This is particularly important in relation to peak flows, both at springs (when resuspension may occur) and neaps (when settling of fines may occur), and also the direction of the residual transport. Wind effects, although typically of secondary importance in this type of flow regime, may be important to the residual transport of the lighter (i.e. finer) sediment fractions. In addition, the modelled release scenario has to consider sediment characteristics (grain size and density) at the time and point of release to appropriately reproduce the effect of the prevailing hydrodynamic and wind conditions on dispersion patterns. Thus, the settling velocity and bulk density of the sediment are important properties in determining the fate of disposed sediment.

In this study, ten independent, realistic disposal scenarios have been modelled based on typical times of dredged release and their results, in combination, reveal the effect of wind strength and direction and the point in the tidal cycle that release occurs has little effect on the eventual fate of the sediment. Worst case scenarios are considered in which the total released sediment is comprised of fines which have a much larger footprint than the coarser sand fraction.

The model results clearly show that relatively coarse sediments (> 500 μm) disposed of at Nab Tower remain within the site, resulting in up to 5 mm of sediment overburden in the direct vicinity of the discharge location. Meanwhile, the ‘fine’ sand fraction becomes resuspended during peak spring tide but, once deposited, remains in local depressions within the site or in the near vicinity to the east. The ‘very fine’ sand fraction is initially deposited along the southwest-northeast trajectory of the tidal excursion, but the strong tides and residual current result in a broad spread of the material, with some sediment being transported out of the model domain. Finally, with respect to the ‘fine’ (i.e. silt) fraction, there is some small immediate local deposition at the disposal site, but the strong tides in the region rapidly resuspend this and redistribute it throughout the model domain, albeit at low concentrations.

In relation to the MCZ, the model outcomes indicate that there does not appear to be either temporary or long-term deposition > 0.5 mm within the designated boundary.

Due to the strong tides in the region, there is no benefit of a tidally related discharge condition, as this would not have an effect on the eventual distribution of material.

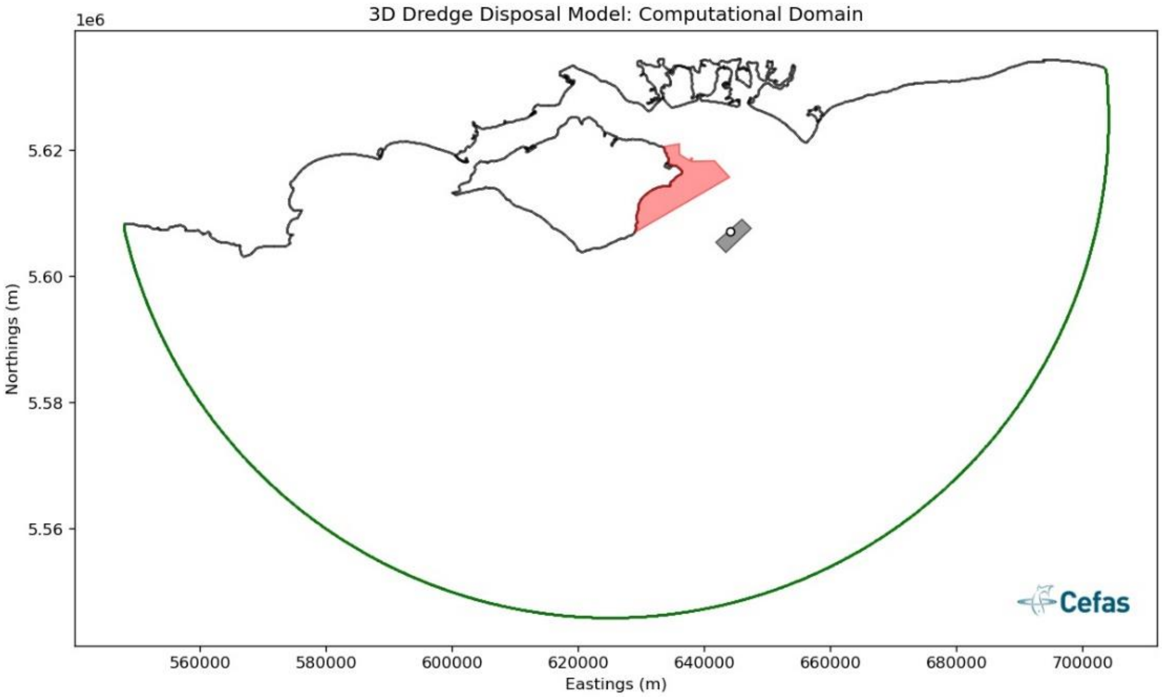

Figure 1 Map showing Nab Tower disposal site (grey rectangle) and the Bembridge MCZ (shaded red), coordinates are UTM. The point of release for modelled scenarios within the disposal site is indicated by the small circle.

Contents

List of Figures

List of Tables

1. Introduction

Nab Tower (NT) is a well-used dredged material disposal site, 30-40 m in depth and approximately 13 km southeast of Bembridge, Isle of Wight. The site is the main disposal location for both maintenance and capital material from ports, harbours, berths and navigational channels in Southampton, Portsmouth and the Isle of Wight. Between 1990 and 2010, over 28 Mt (wet weight) of dredged material were disposed to the site; although the site normally receives 500,000 to 750,000 t per annum, peaks over 1 Mt in 1999, 2001 and 2004 were disposed. The largest capital campaigns were in 1995 and 1996 when 5.3 and 6.3 Mt wet weight (respectively) were disposed, and, more recently in 2014 with the placement of almost 5 Mt of material.

In recent years, there has been several applications for large amounts of material to be disposed to Nab Tower. The most recent of which involved the licensing of approximately 6 Mt (wet weight) of clay, gravel, sand and silt material to the site. To provide data to allow an assessment of the ecological implications of this large deposit, the MMO sanctioned ecological sampling under the auspices of C6794 during 2017 (Bolam et al., 2018); the acquired data described the ecological conditions at the end of this large disposal, with further sampling to assess recovery conducted in 2018 (Bolam et al., 2019).

Currently, there are concerns that the disposal activity at NT is potentially leading to wider impacts as there are anecdotal reports from the local fishing community that bottom gear (e.g., pots) are being smothered by fine sediment and that smothering of benthic habitats within the Bembridge MCZ, situated to the northwest of the site, is a consequence of disposal activity. In response to this, the Marine Management Organisation (MMO) commissioned Cefas to undertake a sediment dispersion modelling study to acquire robust data (via modelled outcomes) regarding the potential for sediment disposed to NT to affect the seabed within the Bembridge MCZ. To ensure the outcomes reflected the realistic disposal regime to the site, the modelling study implicitly required an understanding of the effects of time of disposal (i.e. relative to flood and ebb tide and spring and neap regime), sediment type (variations in the composition of the finer sand fractions) and wind strength and direction. The propensity of these factors to alter the eventual fate of disposed material was included within this modelling study.

2. Methods

2.1. TELEMAC 3D and SEDI-3D: an overview

TELEMAC is a suite of state-of-the-art computational models, composed of many modules. It has been widely applied to model both hydrodynamics and the transport of cohesive and non-cohesive sediment in a coastal environment (Hervouet, 2007). The TELEMAC 3D model has been thoroughly validated over the past 30 years through numerous studies including previous studies of the hydrodynamics around the NT disposal site (HRW, 2012). Hence, the SEDI-3D model within TELEMAC 3D is a model well-suited to estimating the spreading of dredged material, including sediment transport in suspension over the water-column as well as erosion and deposition dynamics of deposits on the seabed.

The 3D σ-grid TELEMAC3D module has been used to replicate flow due to both tidal forcing and the forcing due to surface wind shear. Near-surface sediment release (from the dredger) and subsequent transport over the water-column is resolved in three-dimensions and runs online, i.e., in a coupled fashion, using the SEDI-3D component of the TELEMAC3D module (Hervouet, 2007). SEDI-3D is capable of modelling the evolution of both non-cohesive and cohesive sediments as well as mixed sediments comprising two fractions (one cohesive and one non-cohesive). The focus of this report is specifically on modelling the non-cohesive (sand) and cohesive (fines and silts/muds) fractions of dredged material in order to consider a realistic worse-case dispersal scenario.

2.2. Model setup

The TELEMAC model was set up in 3D using a σ-grid comprising 8 layers in the vertical. The σ-grid is 'topography following'; this facilitates a better representation of both the surface shear processes from wind and the near bed deposition and resuspension processes. The turbulence closure scheme used was the Tsanis vertical mixing length model (Tsanis, 1988). The background vertical viscosity was set to 1 x 10^{-4} m^2 s^{-2}. No thermal or freshwater effects are included into the density structure. Following the previous work described in the SCDA MAREA Report (HRW, 2012), the inclusion of temperature and salinity gradient effects for this area was deemed unnecessary; an assumption that is supported by the excellent hydrodynamic validation results. The sediment is released at a depth of 7 m in the model to provide a reasonable estimate of likely dredger release (i.e. typical draft of the dredging vessel – UKD MV Blue Fin is 6.7 m). Wind is modelled via a forcing term that appears in the equations through the two-dimensional condition at the surface.

A constant value of 1.3 kg m^{-3} is used for the wind-induced friction on the free-surface. The wind velocities are assumed to be given at 10 m above the water surface. The model utilises the wind speed varying drag coefficient of Flather (1976). This wind drag coefficient parametrizes a number of complex physical process, and, is itself, a function of the existing wave climate and wind speed.

2.3. Mesh creation

A new unstructured mesh has been created specifically for this modelling work. The mesh comprises 998,144 (~ 1 M) computational nodes distributed over 8 vertical layers. The mesh includes the following considerations:

- Spatial extent: the model domain extends from Weymouth in the west to Brighton in the east, incorporating the Isle of Wight, and is sufficiently large to properly capture both wind and tidal effects. Moreover, careful consideration has been given to the offshore boundary which is subject to tidal forcing. This boundary has been defined as an arc to enable smooth transitions of both the water levels and velocities employed for the forcing.

    - Mesh structure: the unstructured mesh comprises a Delaunay triangulation of points: these are extruded in the vertical according to a topography following a σ-grid structure.
    - Refinement and cell size: in the vicinity of the disposal site, as well as at the boundaries and the shorelines, the mesh has been refined. Validation locations fall within the refined areas of the mesh, enabling a better resolution of the flow dynamics in these key locations. The edge length of the computational cells ranges from 20.8 m to 2.2 km depending on the level of local refinement; the mean edge length in the model is 202.5 m. In the model, the sediment discharge is prescribed as a point source that is distributed over one computational element. As the dredged material release occurs over a short timeframe, the spatial location of the dredged material release is assumed to be fixed. A visual

representation of the mesh that clearly illustrates the local refinement is given in Figure 2.

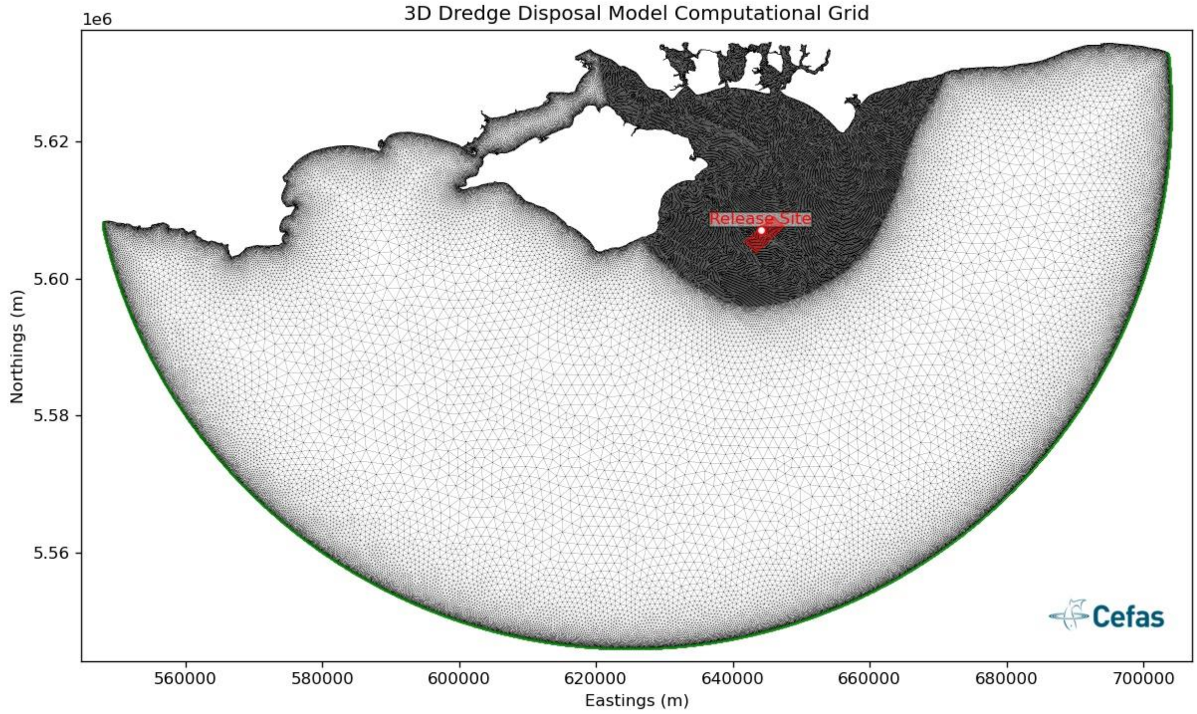

Figure 2 The TELEMAC3D unstructured mesh used in the modelling showing the localised refinement around the disposal site, shoreline and tidal boundaries. The tidal boundary is displayed as a green arc. The release point within the Nab Tower disposal site is also indicated.

2.4. Bathymetry construction

Model bathymetry is based on a Digital Elevation Model (DEM) with a resolution of six arc-second, created by Astrium (Astrium, 2011), with bathymetry around the Isle of Wight stemming from hydrographic survey data archived at the UKHO. The vertical datum is Ordnance Datum and horizontal coordinates are UTM zone 30N.

2.5. Tidal-boundary conditions implementation

The seaward boundary of the model (which takes the form of an arc in the model in order to allow for smooth variation across the model domain; Figure 2) is a tidal boundary. The use of an arc for this boundary avoids discontinuous transitions associated with corners. To recreate the tidal signal at the boundary via superposition it is necessary to have knowledge of the harmonic constants. Thus, at the tidal boundary, information has been extracted from Topex Poseidon Satellite Altimeter (TPXO) model data (https://www.tpxo.net/global) giving the following principal harmonic constituents: M2, S2, N2, K2, K1, O1, M4, MS4.

2.6. Implementation of the behaviour of dredged material

According to the sampled dredged material, the sediment particle size distribution is composed of two main components: sand and silt fractions, in an approximate proportion of 30% and 70%, respectively. Both respective fractions are made up of a range of grain sizes that correspond to these sediment class, i.e., non-cohesive or cohesive sediment. In the modelling presented here, to determine a conservative disposal footprint, we focus individually on the sand and silt fractions in a worst-case scenario. Shear stress independent deposition is employed in the model in order to adequately account for grain sizes that are larger than the median prescribed value from which the settling velocity is assumed. A critical bed shear stress is employed for erosion. The critical bed shear stress for silt is almost constant as shown in Soulsby (1997). The parameters set up for the silt-like sediment are given in Table 1.

The settling velocity of sediment was dictated by the sediment type. For the silt fraction and small grain size classes, Stokes' Law can be used to calculate the settling velocity (Soulsby, 1997). For the sand fraction, viscous forces continue to play an important role in the settling behaviour; however, the departure from Stokes' Law is significant enough that wake turbulence cannot be ignored. With this in mind, the empirical relationship of Ferguson and Church (2004) is employed in the model to compute the settling velocity of the larger, non-cohesive sediment fraction. Figure 3 illustrates the effects of grain size on settling velocity for both Stokes' Law and the empirical relationship of Ferguson and Church (2004). Moreover, as almost immediately after release the cohesive sediment disperses and concentrations become less than 200 mg l^{-1}, the settling velocity of the cohesive fraction was assumed to be insensitive to sediment concentration. This assumption is in accordance with standard practice (Smolders et al., 2018), see Table 2.

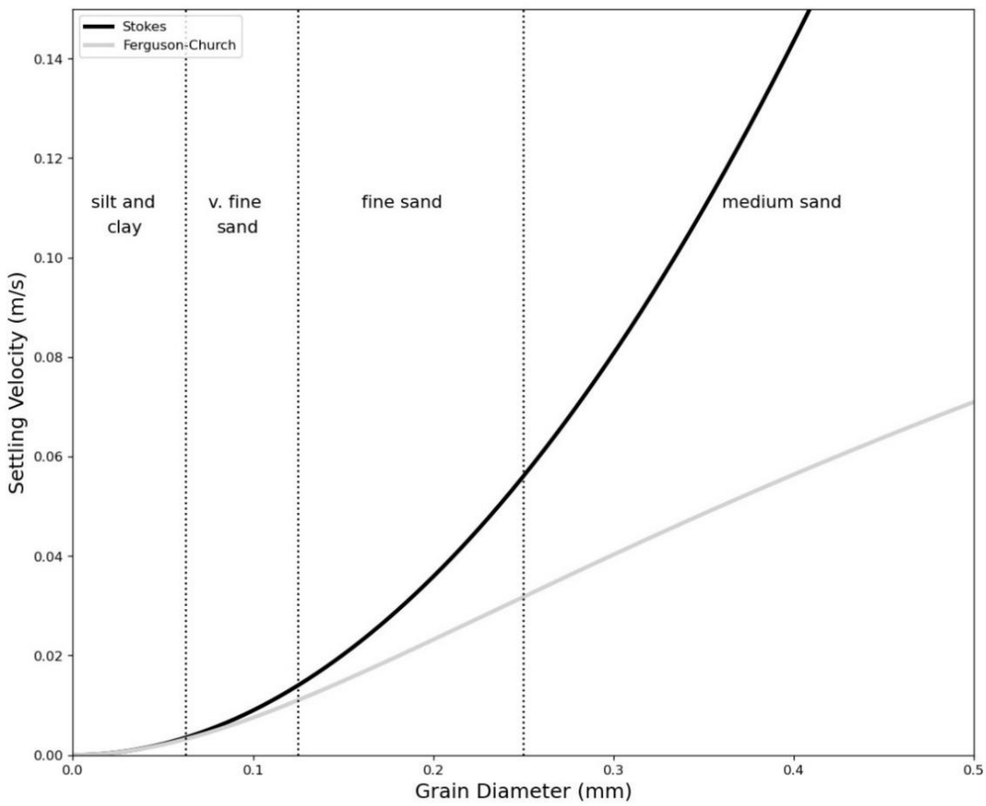

Figure 3 Settling velocity as a function of grain size for the various sediment fractions.

Independent sediment transport and morphological updating modules were employed for the cohesive and non-cohesive sediment components. For the cohesive (fine) sediment fraction, deposition *D* was modelled as a shear stress independent flux. This approach is in line with recent work involving the modelling of cohesive sediment transport (see, for example, Smolders et al., 2018 who also employed SEDI-3D). This is achieved here by setting a large value (1,000 Pa) for the critical mud shear stress in the 3D model. Interaction of sediment in suspension with the seabed are reproduced with erosion (Em) and deposition (Dm) fluxes, calculated with the following Krone-Partheniades formulation (Partheniades, 1965) (cf. Salehi and Strom, 2012):

$$F_m = E_m - D_m = M_m\left(\frac{\tau_b}{\tau_{e,m}} - 1\right)H\left(\frac{\tau_b}{\tau_{e,m}} - 1\right) - w_m c_m\left(1 - \frac{\tau_b}{\tau_{d,m}}\right)H\left(1 - \frac{\tau_b}{\tau_{d,m}}\right)$$

Where

F_m	Mud flux from the bed to the water column
E_m	Erosion flux of mud
D_m	Deposition flux of mud
M_m	Erosion coefficient for mud beds
D_m	Deposition flux of mud
$\tau_{e,m}$	Critical erosion shear stress for mud
$\tau_{d,m}$	Critical deposition shear stress for mud
H	Heaviside function, $H(f(x)) = 1$ if $f(x) \geq 0$, otherwise $H(f(x)) = 0$

Table 1: Impact of sediment concentration on settling velocity (from "Properties of dredged material, HRW, Report TR54, June 1998 – see also Cuthbertson et al. 2008)

Fine-grained concentration [mg l^{-1}]	**Impact on settling velocity**
1-200	Insensitive to concentration
200-5,000	Enhanced settling velocity with concentration
>5,000	Hindered and reduced velocity with increasing concentration

In the case of the non-cohesive sediments, the erosion flux can be expressed in terms of an equilibrium reference concentration, and the deposition flux is calculated as the product of settling velocity w_s and near-bed concentration C_0.

The vertical profile of the suspended sediment concentration is treated as a passive scalar and can be determined by solving a classical transport/diffusion equation, with an additional vertical advection term that represents the effect of the gravitational settling velocity.

At the free surface (Zs), the net vertical sediment flux is set to zero:

$$\left(\nu_t \frac{\partial c}{\partial z} + w_s c \right)_{z=Z_s} = 0$$

Whilst at the bottom, a Neumann-type boundary condition is specified, in which the total vertical flux equals the net erosion (E) minus deposition rate (D):

$$\left(\nu_t \frac{\partial c}{\partial z} + w_s c \right)_{z=Z_b} = D - E$$

To obtain the evolution of the bed (Z_b), due to deposition/erosion of deposited sediments:

$$C_b \frac{\partial Z_b}{\partial t} = D - E$$

When a uniform bed of concentration C_b (cohesive sediment) or $C_b=(1-\chi)$, where χ is the bed porosity (non-cohesive sediment), is considered.

Here, the conservative N-Scheme (Hervouet, 2007) is employed for the advection of the sediment thus ensuring that the model properly conserves sediment mass. The split horizontal-vertical advection-diffusion-settling scheme of Benson et al. (2014) is employed to model the sediment motion and deposition.

In summary, the disposal has been implemented in the model as a single representative cohesive silt fraction and three distinct non-cohesive (sand) fractions to present a reasonable worst-case scenario. Both the cohesive and non-cohesive fractions are prescribed by a representative mean diameter, specific density as well as a representative settling velocity. For the cohesive fraction, a specific critical shear stress and erosion parameter are employed. For the non-cohesive sediment, the equilibrium concentration formula provided by Zyserman and Fredsoe (1994) is employed for the reference concentration. For both sediment types, a representative wet density is employed to calculate the release volume at the NT site. The sediment is released as a point source over a computational element at a depth of 7 m below the free surface. Details relating to the sediment properties used in the modelling are provided in Tables 2 and 3.

Table 2: Cohesive sediment characteristics of the representative silt fraction released in the model.

Representative silt fraction	
Mean Grain Diameter (μm)	50
Erosion parameter Mm [kg m^{-2} s^{-1})]	0.0001
Critical Deposition Shear Stress [Pa]	1000
Wet density [kg m^{-3}]	1250
Particle specific density [kg m^{-3}]	2700
Settling velocity [mm s^{-1}]	0.5
Critical Erosion Shear Stress [Pa]	0.05

Table 3: Non-cohesive sediment characteristics of the three representative sand fractions released in the model.

Representative sand fractions (very fine, fine, medium)	
Mean grain diameter (μm)	125; 250; 500
Wet density [kg m^{-3}]	2,000; 2,000; 2,000
Particle specific density [kg m^{-3}]	2,650; 2,650; 2,650
Settling velocity [m s^{-1}]	0.01; 0.03; 0.07
Shield's Parameter [-]	0.047; 0.047; 0.047

3. Calibration and validation

After the model had been set up, a process that involved several iterations of the mesh and tuning of the physical parameter settings, initial calibration was preformed against water levels at selected tide gauges within the model domain. The tide gauges were selected in order to cover the widest geographical range within the model domain and, thus, provide a comprehensive check of the overall model performance. Once calibration against elevation had been undertaken, the model was then validated against a different data set for elevation and velocity.

3.1. Elevation calibration

Whilst the TELEMAC 3D model has been extensively validated for use in both marine and coastal environments it is always prudent to conduct a localised calibration and validation of the model. Thus, to give further confidence in the model results, hydrodynamic predictions obtained using the model have been validated. The first stage of the model validation is in terms of the free surface tidal signal at four coastal locations within the model domain. Specifically, the tide gauges at Lymington, Portsmouth, Bournemouth and Sandown Pier were utilised. These four gauges give good spatial coverage over the model domain enabling a high confidence in the elevation calibration. Observed data were downloaded from the Sea Level Station Monitoring Facility website (http://www.ioc-sealevelmonitoring.org/) for each of these tidal gauge stations. This calibration test checks that the tide propagates through the entire model domain from the boundary correctly to confirm that the mesh is of sufficient resolution and the physical/numerical parameters are suitably adjusted. Results are presented here (Figure 4) for the first seven days of January 2020. In accordance with previous modelling work (HRW, 2012) and to facilitate comparison with the observed data, individual offsets were applied at each of the gauges to normalise the reference level between the modelled and observed data.

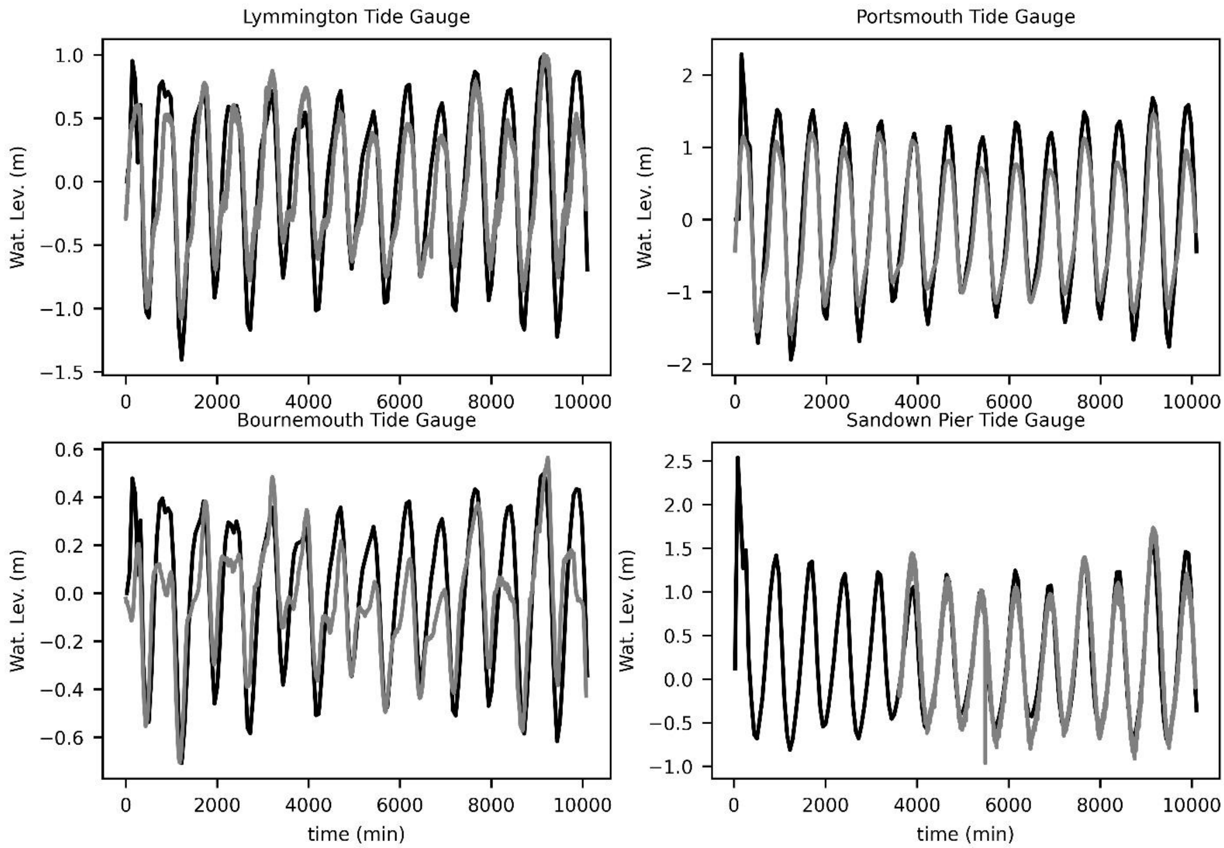

Figure 4 Comparison of modelled (black) and observed (grey) free surface time series at several distinct locations within the computational domain.

It can be seen that, with the exception of the Bournemouth tide gauge, the model results for the water level time series are in excellent agreement with the observations. The most apposite for comparison in this work is the Sandown Pier gauge where the agreement between the modelled and observed tidal signals is clearly excellent. The discrepancy at Bournemouth is most likely due to local, small scale bathymetric and meteorological effects that produce an unusual tidal curve. Moreover, the mesh resolution is relatively coarse in this location and, as the location is sufficiently removed from the area of interest, these discrepancies do not warrant further investigation here.

3.2. Elevation validation: spring tide

Without any additional adjustment, the calibrated 3D model was validated against time-series data at the NT site for both water levels (tide qauge SCDA2) and currents. The results from the SCDA2 gauge for the spring tide are shown in the top panel of Figure **7**. In agreement with the findings of HR Wallingford (HRW, 2012) a comparison of the modelled and measured depths indicates a difference in the bathymetry at this location; on average the modelled seabed at this location is 1.9 m above the measured value. This difference is likely to be the result of inaccuracies in the bathymetric data used in the numerical model (the bathymetric dates from 2011) and/or because the seabed contours in the vicinity of the measurement site are not closely represented by the linear interpolation in each triangular cell of the finite element mesh. It is worth noting that there are mobile sand waves on the seabed in this part of the eastern Solent, so that these differences in depth may simply be due to short-term variations changes in bed levels. To facilitate comparison of the measured and predicted rise and fall of the water levels at this site, a simple correction has been applied to the model results in the top pane of Figure 5, i.e. the output water depths have been increased by 1.9 m. This shows a close agreement between the data sets, with only a slight under prediction of high tide levels being evident in the model results. The model over predicts the tidal depth range by approximately 10% compared with the observed values.

3.3. Elevation validation: neap tide

The results from the SCDA2 gauge for the neap tide are shown in the bottom panel of Figure 5. As is the case for the spring tide, to facilitate comparison of the measured and predicted rise and fall of the water levels at this site, the same correction has been applied to the model results in the bottom pane of Figure 5, i.e. the output water depths have been increased by 1.9 m. The bottom panel of the Figure shows the model output predictions for the water depths in the neap tide including the period for which observed data were available. A comparison of the modelled and observed data shows a close agreement between the data sets with the model over-predicting the tidal depth range by <5% compared with the observed values.

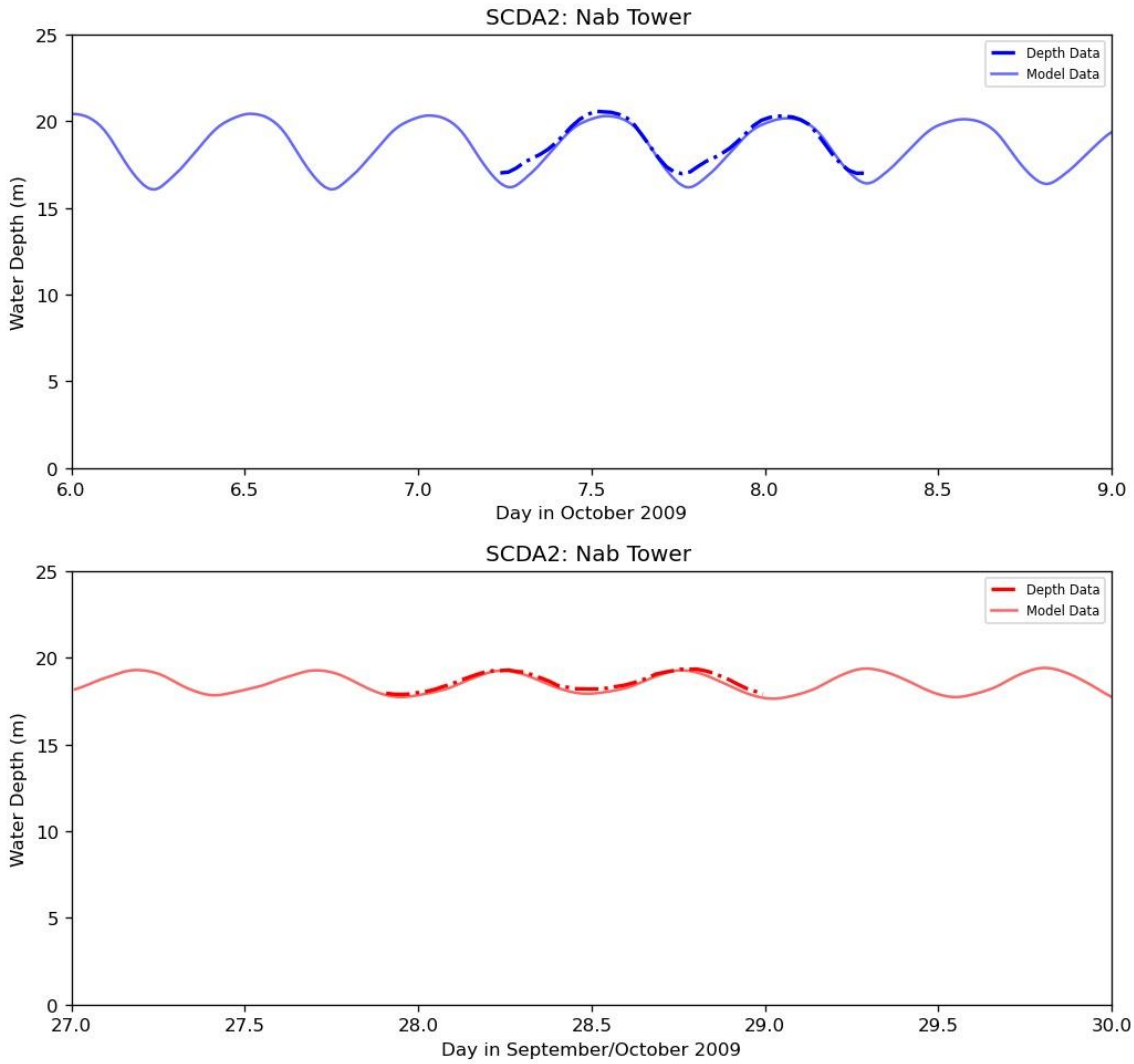

Figure 5 Comparison of predicted (with correction) and observed water depth (dotted line) at the Nab Tower disposal site for a Spring tide (top) and Neap tide (Bottom).

3.4. Velocity validation: data source

The second stage of testing involved checking the prediction of currents close to the NT disposal site. Figure 6 shows a snapshot of the instantaneous depth-averaged currents in the vicinity of the disposal site and provides an insight into the flow patterns and velocity magnitude in the area of interest.

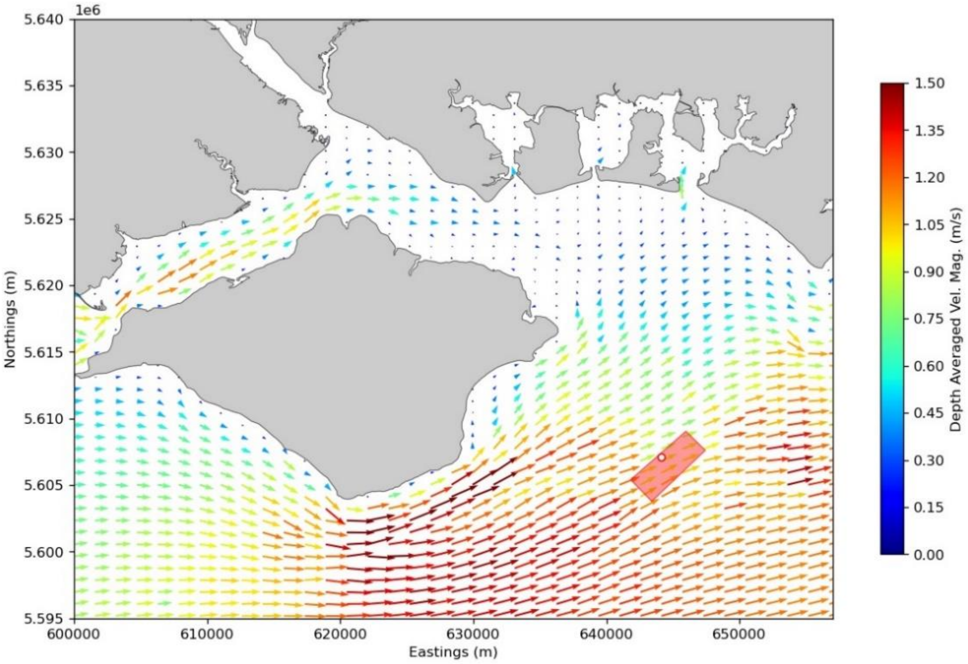

Figure 6 An example of the modelled instantaneous depth-averaged currents in the vicinity of the Nab Tower disposal site (denoted by a transparent pink rectangle).

Data sets for validation at this site are limited; indeed, the only suitable data set found for comparison was that presented in the SCDA MAREA report (HRW, 2012). The SCDA2 data set comprises a total of 5,679 current records spanning the period 21/09/2009 11:30 to 14/12/2009 09:30, recorded using 1 MHz Nortek AWAC deployed at position 644417 m E, 5614454 m N (UTM30N) which is approximately 7 km north of NT. Further information relating to the data, and the data collection methods, can be found in the SCDA MAREA report (HRW, 2012). Following the work presented in the MAREA report (HRW, 2012), two periods, corresponding to periods of spring and neap tides, were employed for comparison in the present study. Period 1 extends between 07/10/2009 05:30 and 08/10/2009 07:00 and corresponds to a spring tidal cycle whilst period 2 extends between 27/09/2009 22:50 and 29/09/2009 00:20 and comprises a neap tidal cycle.

3.5. Velocity validation: spring tide

Figure 7 provides a comparison of the simulation results with the depth-averaged time-series of the U and V components derived for the observed time-series for the spring period. The observed time-series was obtained through digitizing the EMU ADCP data provided in Figure 2.5 of the "*MAREA: Flow and Wave Model Validation*" report (HRW, 2012). The quantity U is the easterly component of flow while V is the northerly component of flow. It can be seen from Figure 7 that the model results are in very good agreement with the observations. The U component is approximate twice the V component, the root mean square error (RMSE) of 0.06 m s^{-1} for U (peak flows of 0.8 m s^{-1}) confirms that the model is predicting the flow speeds with a high degree of accuracy. The observational record for V is potentially unreliable as it is not centred on zero implying a strong northerly residual. The neap tide record shows a clean, evenly matched north – south component. The U velocity data are extremely well replicated by the model, so it is difficult to reconcile such a good fit to the U component and its associated clean tidal signal (implying little meteorological influence) and the apparent offset in V velocity of the ADCP data. In conclusion, there is there is probably an artefact (mostly likely in processing) of the depth-averaged V velocity data.

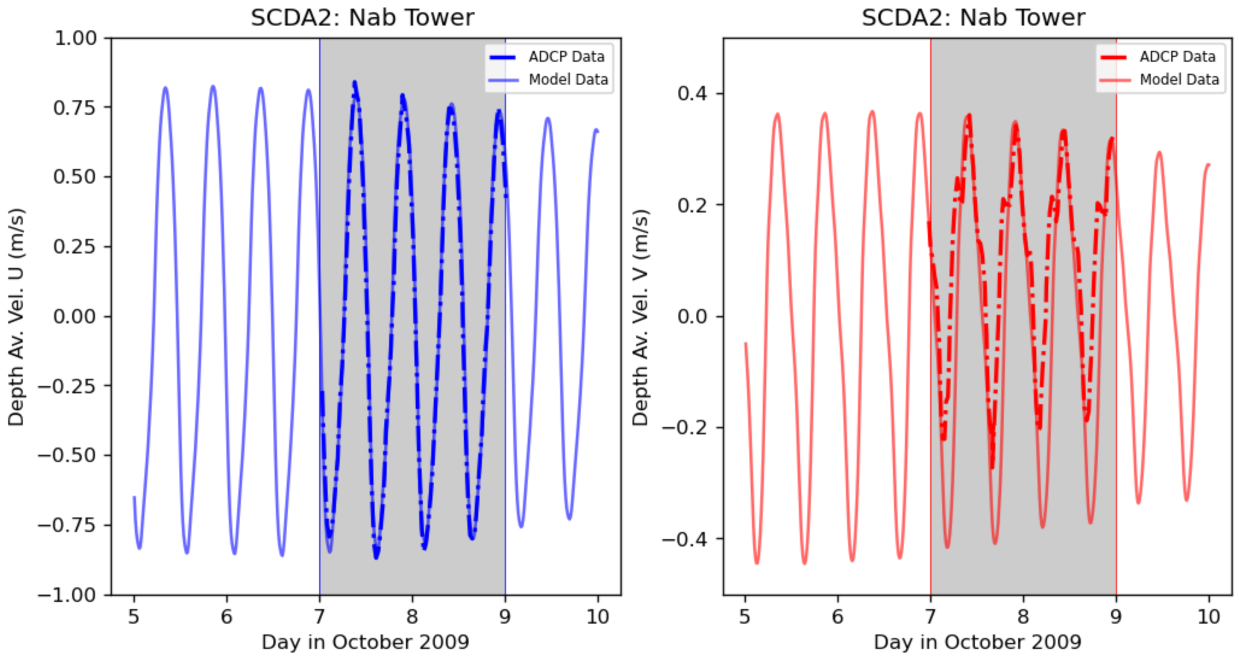

Figure 7 Comparison of modelled and observed (ADCP data) depth-averaged tidal currents at the Nab Tower disposal site for a spring tide.

3.6. Velocity validation: neap tide

Figure 8 provides a comparison of the simulation results with the depth-averaged time-series of the U and V components derived for the observed time-series for the neap period. Again, the observed time-series were obtained through digitising the EMU ADCP data provided in

Figure 2.6 of the "*MAREA: Flow and Wave Model Validation"* report (HRW, 2012). It can be seen from the Figure that the model results are in very good agreement with the real-world observations. Importantly, for the majority of the validation period, the model slightly over-predicts the depth-averaged easterly and northerly velocity component meaning that any estimations of the disposed sediment footprint based on model results are likely to be conservative. The RMSE of 0.05 m s^{-1} for U and 0.04 m s^{-1} for V confirms that the model is predicting the flow speeds with a high degree of accuracy.

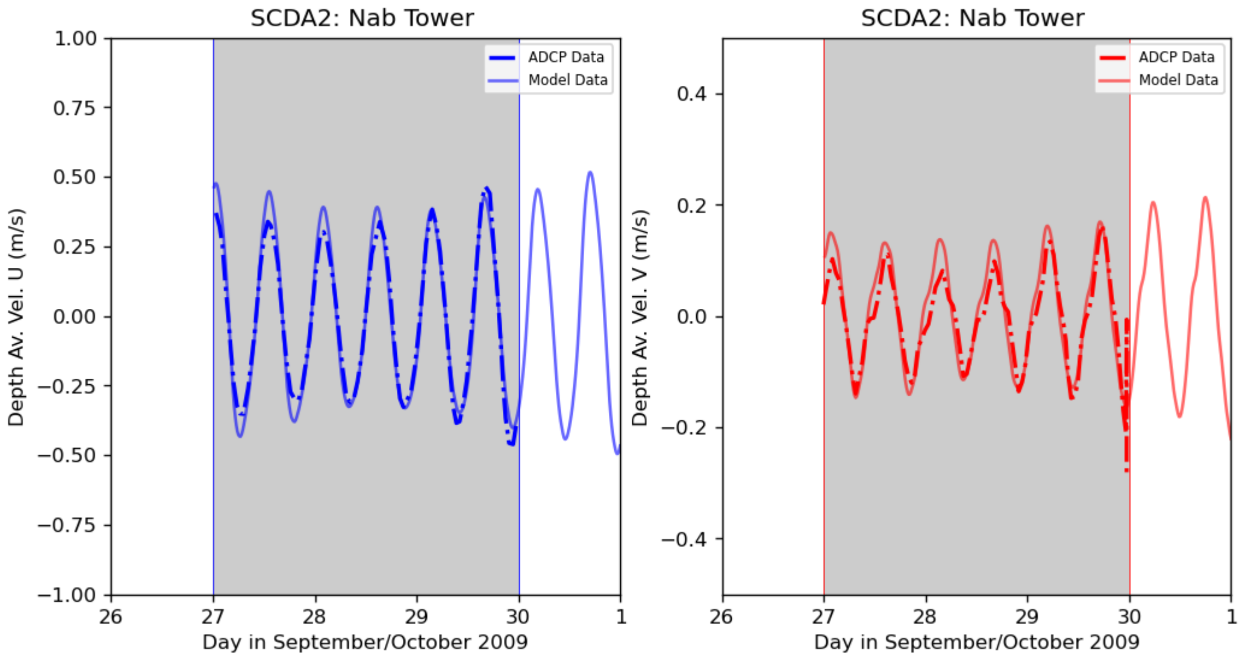

Figure 8 Comparison of modelled and observed (ADCP data) depth-averaged tidal currents at the Nab Tower disposal site for a neap tide.

3.7. Summary of calibration and validation

The comparison of modelled and observed hydrodynamic data for both the water level and the depth-averaged current components gives a high degree of confidence in the 3D model developed here. As the validated currents are in the immediate vicinity of the disposal site, this validation consolidates the high degree of confidence in the ability of the 3D model to make predictions of the fate of the disposed sediment.

It should be noted that the model cannot predict the meteorological conditions which affect the observed currents or elevations; moreover, the model uses bathymetric data that were acquired at a specific date and resolution. Thus, differences between the model predictions and the observed data are likely to be a result of combined bathymetric and meteorological discrepancies between the model and reality.

4. Scenarios

In the present study, we consider ten independent scenarios for the disposal of dredged sediment. In all scenarios, all sediment is assumed to be either one of three representative sand fractions or a single fraction of fines (silt) which facilitates the spreading of the sediment to maximise the deposition footprint. This means that a total of four representative sediment classes are considered, namely: silt (50 µm); very fine sand (125 µm); fine sand (250 µm); and medium sand (500 µm). Each of the ten scenarios has been selected to test a specific hypothesis regarding the effect of timing of disposal and wind strength and direction on eventual fate of the material on the seabed. These were deemed to represent plausible licence conditions which may be considered for disposal to NT should the model indicate there was a possibility (under certain conditions) that disposed material resulted in a significant deposition overburden within the MCZ. Table 4 lists the various modelled scenarios as well as the rationale behind them.

One of the potential management options to be investigated is related to the time of release in relation to high water, i.e., can release time form the basis of a licence condition to reduce potential impact to the Bembridge MCZ? Scenarios 1-6 were designed to address this particular aspect. Scenarios 7-10, meanwhile, address the question of the effect of wind on the sediment plume.

Table 4: Disposal scenarios modelled in the present study

Scenario	Description	Rational/hypothesis	Comments
1	HW	Is timing of disposal significant?	(at a Spring tide, no winds)
2	Disposal at HW +2 hours		
3	Disposal at HW +4 hours		
4	Disposal at HW +6 hours		
5	Disposal at HW +8 hours		
6	Disposal at HW +10 hours		
7	Disposal with strong NW wind (from). U 4.14 m s^{-1} V – 4.14 m s^{-1}	Does wind impact the fate of material up/down the Solent?	Using disposal at 12:00 pm to average over previous disposal times
8	Disposal with strong SE wind U -3.19 m s^{-1} V 3.19 m s^{-1}		
9	Disposal with strong SW wind U 5.22 m s^{-1} V 5.22 m s^{-1}	Can sediment impact on the nearest shoreline?	Using disposal at 12:00 pm to average over previous disposal times
10	Disposal with strong NE wind U -4.74 m s^{-1} V – 4.74 m s^{-1}		

Wind data were sourced from the Meteoblue website[1] with the wind rose given in Figure 9 showing the predominant SW/SSWerly winds. These have been converted into steady state equivalents (90% quartile) as shown in Table 5. As a conservative estimate the winds were considered to be constant for the entire 30-day simulation period.

Table 5: Wind speed estimates 90th centile wind speed estimates

Wind Direction (from)	Wind Speed (mph, m s^{-1})
SW	16.5 mph , 7.37 m s^{-1}
NE	15 mph, 6.7 m s^{-1}
NW	13.1 mph, 5.85 m s^{-1}
SE	10.1 mph, 4.5 m s^{-1}

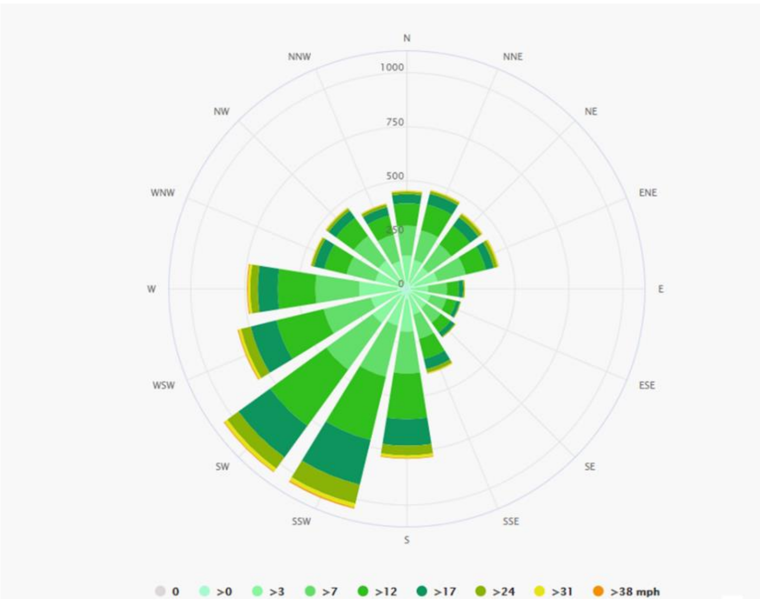

Figure 9 Wind Rose from Ventnor, Isle of Wight.

[1] https://www.meteoblue.com/en/weather/historyclimate/climatemodelled/ventnor_united-kingdom_2634985

4.1. Worst-case disposal volume

The monthly aggregated (from many small) disposal volumes from 2016 to 2019[2] (a total of 274 loads) are shown in Figure 11. The cumulative monthly amounts vary considerably during this four-year period from a maximum of 650,000 m^3 in April 2017 to many months of no disposal. One of the challenges in investigating this data is to distinguish the difference of the impact of capital dredge campaigns and maintenance dredges. Typically, capital dredge material consists of material which is not highly erodible and therefore not likely to spread throughout the system. In contrast, maintenance material tends to have a much higher silt and fine fraction element which can be relatively easily advected from the disposal site, but volumes are generally much lower.

The balance required for the modelling scenario is to select a reasonable worst (but not extreme) case which combines a sediment characteristic (similar to maintenance) which could be a reasonable worst case from a sediment movement perspective.

As noted in section 2.3, the likely fraction of material disposed from a maintenance campaign is 70% fines (silts) and 30% sand, although during high volume capital campaigns that the sand fraction will be higher. Thus, 200,000 m^3 was chosen as a monthly total for the fine material, with 60,000 m^3 chosen for each of the three sand fractions, i.e., a total of 380,000 m^3. There are only 4-months in the 48-month record where disposal was greater than this.

The total monthly amount is made up of individual loads and most loads were under 5,000 m^3, with 194 loads presenting 70.9 % of all the loads disposed at Nab Tower in this period (i.e., many small discharges). Therefore, simulating the total monthly amount as evenly spread over the month would seem appropriate.

[2] 2019 is the latest record available.

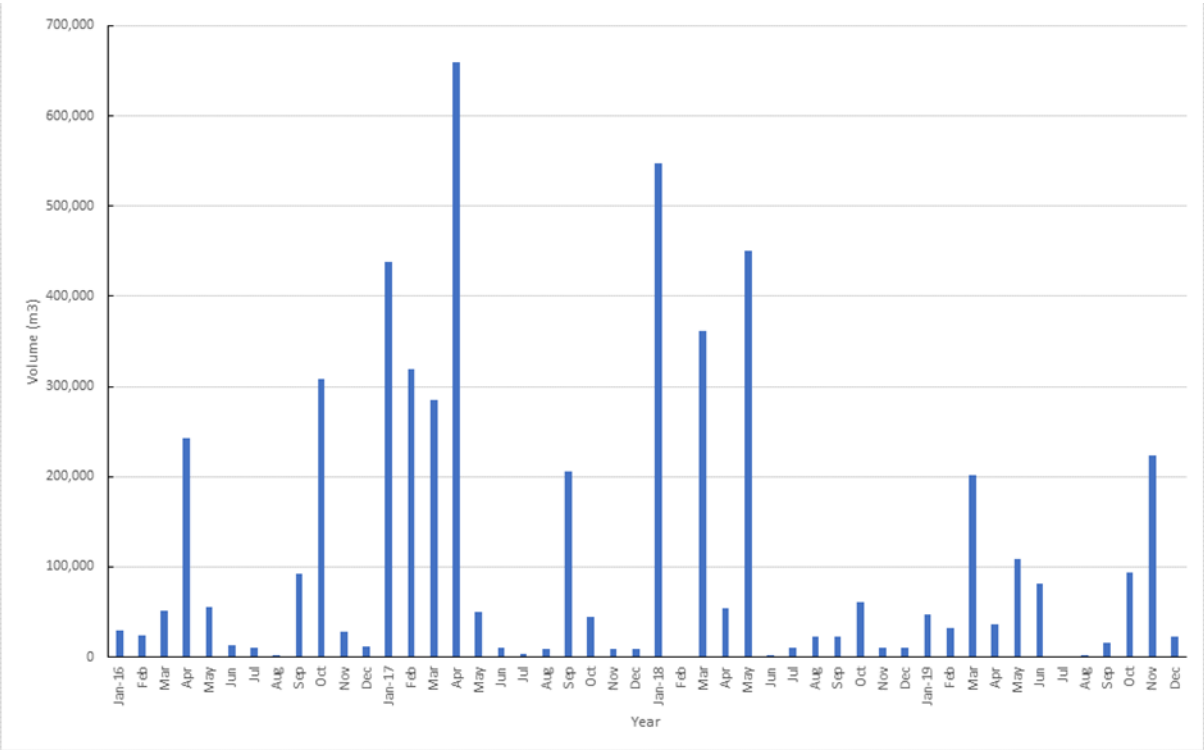

Figure 10 Monthly disposal volumes disposed of at the Nab Tower during 2016 to 2019.

5. Results

In this section, selected results of the modelling are presented. The results are chosen to illustrate the reasonable worst-case scenario associated with the disposal of dredged sediment at NT. A realistic worse-case scenario in which 380,000 m^3 of sediment are released over the month is considered. Approximately, 70% of the disposal was likely to be fines, with 30% of sand fraction (non-cohesive). In the case of non-cohesive sediment, three different sand fractions were considered. For each of the three sand fractions, 60,000 m^3 was released. In the case of cohesive sediment, a single representative fraction was used of 200,000 m^3 released. In all cases, sediment disposal occurs at a depth of 7 m over a disposal period of 10 min. A total simulation period of 30 days is considered, with daily release at different stages of the tidal cycle, with the tidal forcing corresponding to the entire month of April 2020. As the release period is of such short duration (10 min) the release vessel remains in a fixed in position (644099.51 E, 5607131.65 N) and not assumed to move with the tide. The results are presented to form a meaningful narrative regarding the fate of the disposed sediments in terms of sediment overburden at the bed.

5.1. Disposal of Cohesive Sediments (Scenarios 1-10).

Scenarios 1-6 address the potential management option of the time of release in relation to high water.

In this section the fate of fine sediment, is considered. The results, presented in Figure 11, show the depositional footprint over a month for Scenarios 1 to 6 (each comprising a different release stage of the tidal cycle), sampled at an hourly rate with shaded contours between 0.5 mm and 5.0 mm sediment overburden at the bed. Sediment resuspension has a very significant effect, and the mobilisation of the freshly deposited sediment is clearly the dominant factor in determining the fate of the released fine sediment. Analysis of the numerical results show that the residence time for the fine fraction on the bed is short, typically of in the order of minutes. Due to re-suspension, the fine sediment becomes widely distributed throughout the model domain with some sediment being advected out through the model boundaries. It is important to note that the plot shows a 'footprint'; that is, it shows the maximum deposit of sediment observed at a fixed location over the entire monthly period. Due to erosion, the footprint is relatively small as the silt fraction is rapidly dispersed over a large area by the action of the tidal currents. In all cases, based on the results obtained from the hourly footprint, only a very small area in Scenarios 3, 4 and 6 remains covered in sediment. Most likely, what is occurring is that the initial release occurs close to a time when settling can occur. This sediment is then resuspended and then diluted. Scenarios 1, 2 and 5 do not show any sediment deposition footprint, most likely because the timing of release does not directly result in deposition occurring and that when settling does occur, the sediment has been diluted sufficiently that it doesn't accumulate over 0.5 mm.

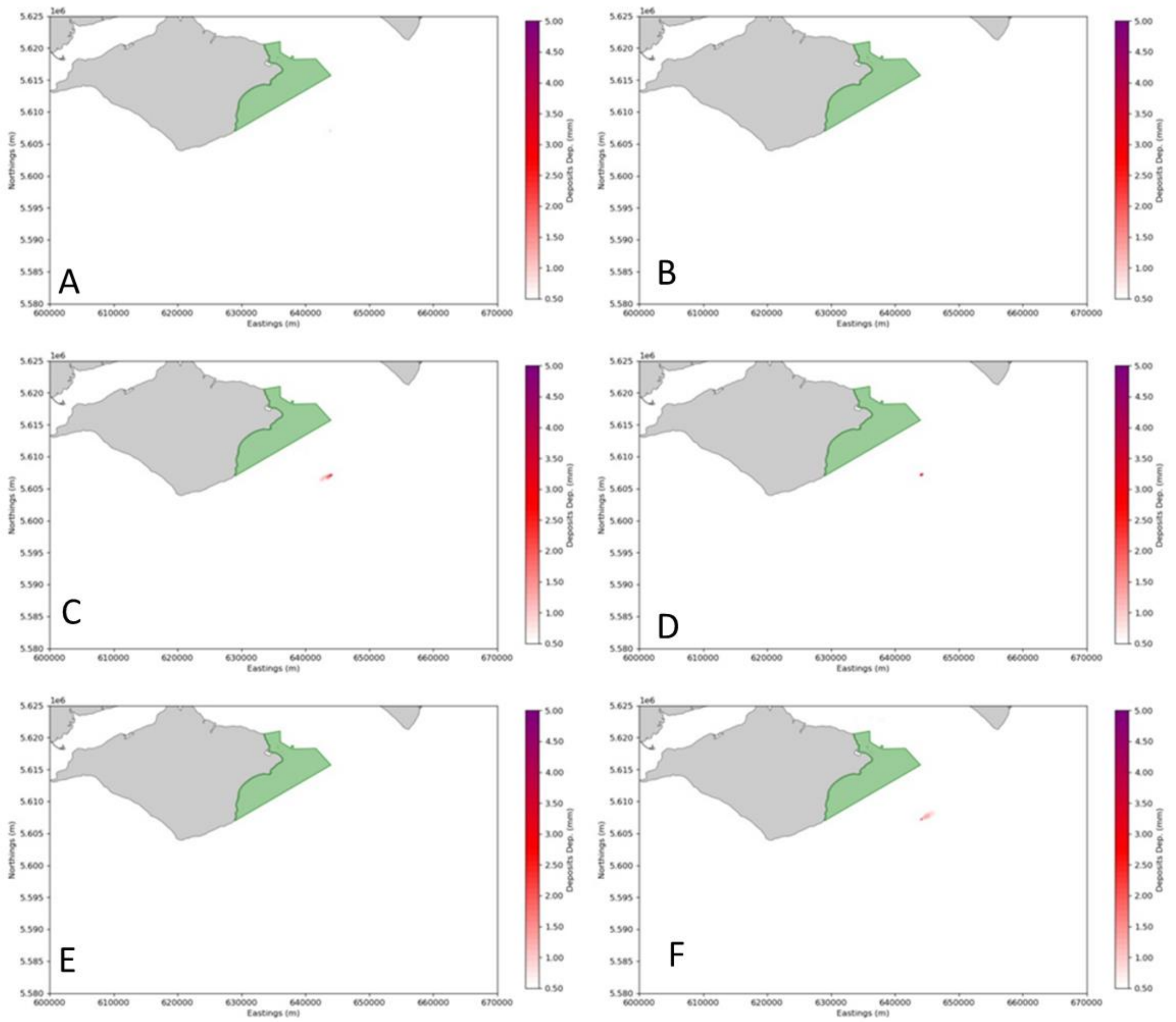

Figure 11 Footprint for Scenarios 1 to 6 . Disposal at HT (A), HT +2 hours (B), HT +4 hrs (C), HT +6 hrs (D), HT +8 hrs (E), HT +10 hrs (F).

Figure 12 presents the results for Scenarios 7-10 which incorporate different winds. The model here uses a daily constant release time of 12:00 pm in order to average the release over different stages in the tidal cycle. Again, the footprint based on hourly sampling is very small and is limited to the vicinity of the disposal site. Evident from the figure is that the wind direction has little effect on the fate of the disposed material. This is most likely due to the strong tides in the region dominating the transport. It should be noted that the winds have been applied as constant winds for the entire period which allows sufficient time for wind-induced currents to develop. This is a conservative approach as, in reality, winds rarely remain in a constant direction for such a prolonged period.

From inspection of animations (not presented) created at hourly intervals, it is evident that there is a passage of fines through the MCZ but these do not settle at depths > 0.5 mm at any time.

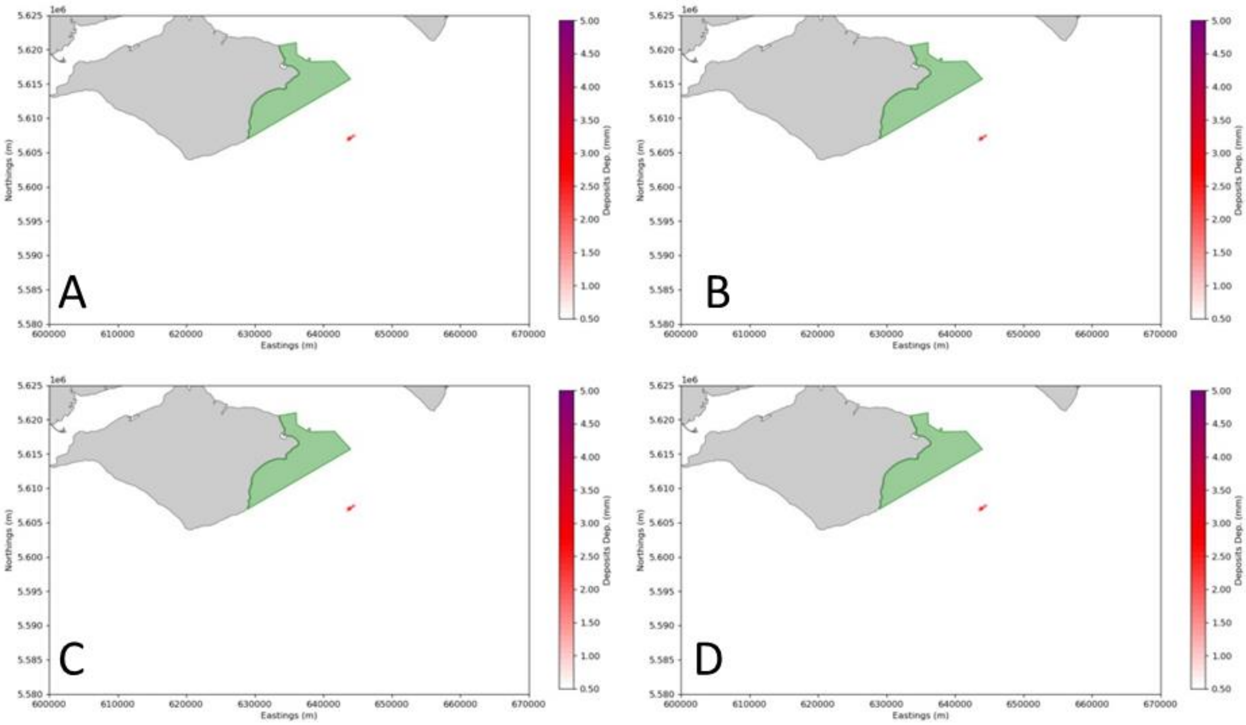

Figure 12 Footprint (based on an hourly samples) for fines (silt) with wind Scenarios 7 (A), 8 (B), 9 (C), 10 (D).

In summary, these results do not show any accumulation of fines settling in the designated boundary of the Bembridge MCZ and this outcome remains regardless of wind direction. As, theoretically, Scenario 8 (SE winds) would be a worst case (winds blowing from the NT disposal site towards the Bembridge MCZ), this wind direction is used for the scenarios for the following coarser sediment fractions.

5.2. Disposal of very fine (125 µm) sand

Analysis of model results (not shown) indicate that Scenario 8 provides the worst-case scenario when considering fate of very fine sand deposited in relation to the location of the Bembridge MCZ. Figure 13 shows the footprint associated with the release of very fine sand for Scenario 8. Again, the footprint is based on an hourly sample rate. The footprint is significantly bigger than that observed for the silt fraction; however, like the silt fraction, the very fine sand is readily dispersed over a large area by the action of the tidal currents. The residual movement of the sediment is again along a north-easterly - south-westerly trajectory with some sediment also being carried away in an easterly direction. Figure 14 shows, by the end of the 30-day simulation period, all the deposited material has been re-suspended and either advected out of the system or, where deposited, sediment overburden is less < 0.5 mm.

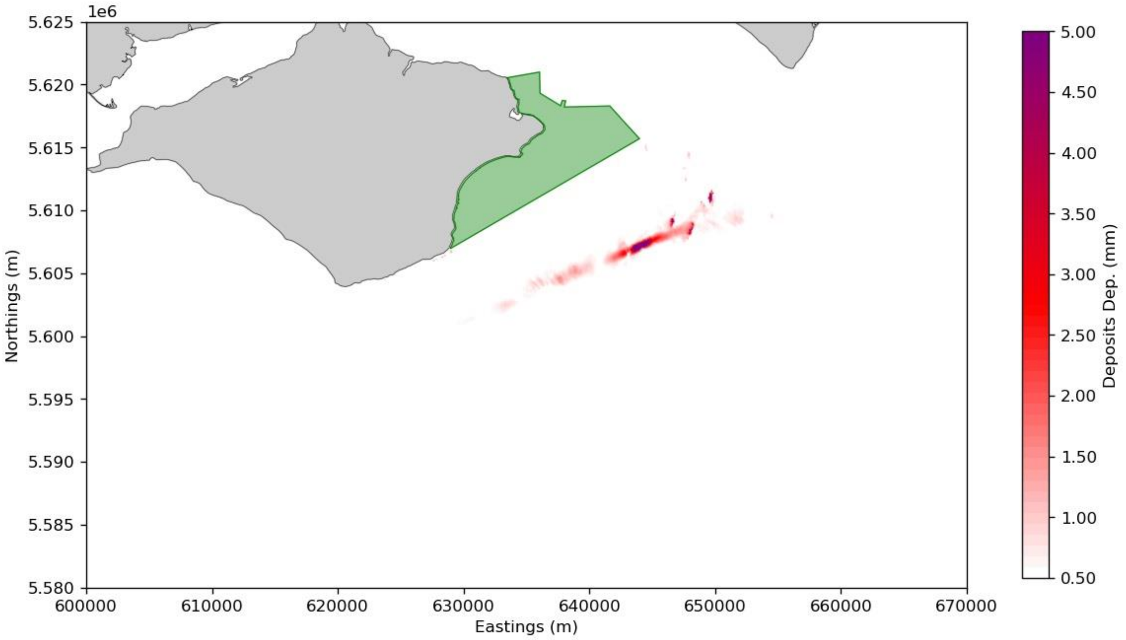

Figure 13 Footprint (based on an hourly sample rate) for non-cohesive very fine (125 μm) sand, Scenario 8.

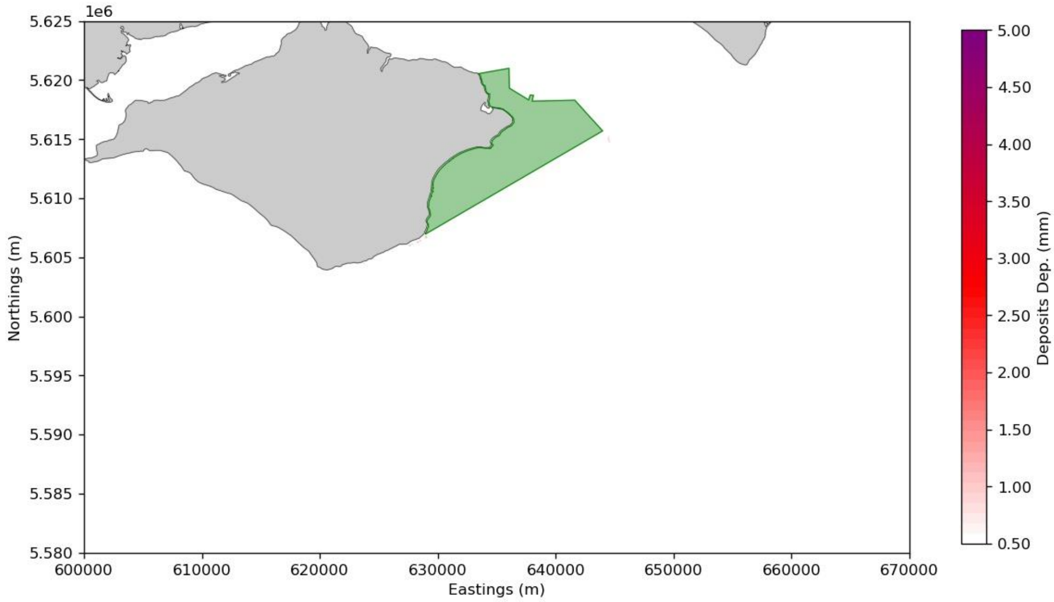

Figure 14 Snapshot of the deposits at the end of the 30-day simulation period for non-cohesive very fine (125 µm) sand, Scenario 8. The figure shows that all sediment was resuspended resulting in zero deposits.

5.3. Disposal of fine (250 µm) sand

Figure 15 shows the footprint associated with the release of fine sand for Scenario 8. For this fraction, the primary residual transport is comparable to that observed for the very fine sand fraction, i.e., north-easterly - south-westerly trajectory with some sediment being transported out of the model domain. The mobility of this fraction is less than that of the very fine sand and consequently the deposits remain somewhat more localised. A snapshot of the sediment deposits at the end of the 30-day model simulation (Figure 16) shows that the sediments disperse much more slowly from the deposition site than very fine sand and mostly remain in the vicinity of the disposal site.

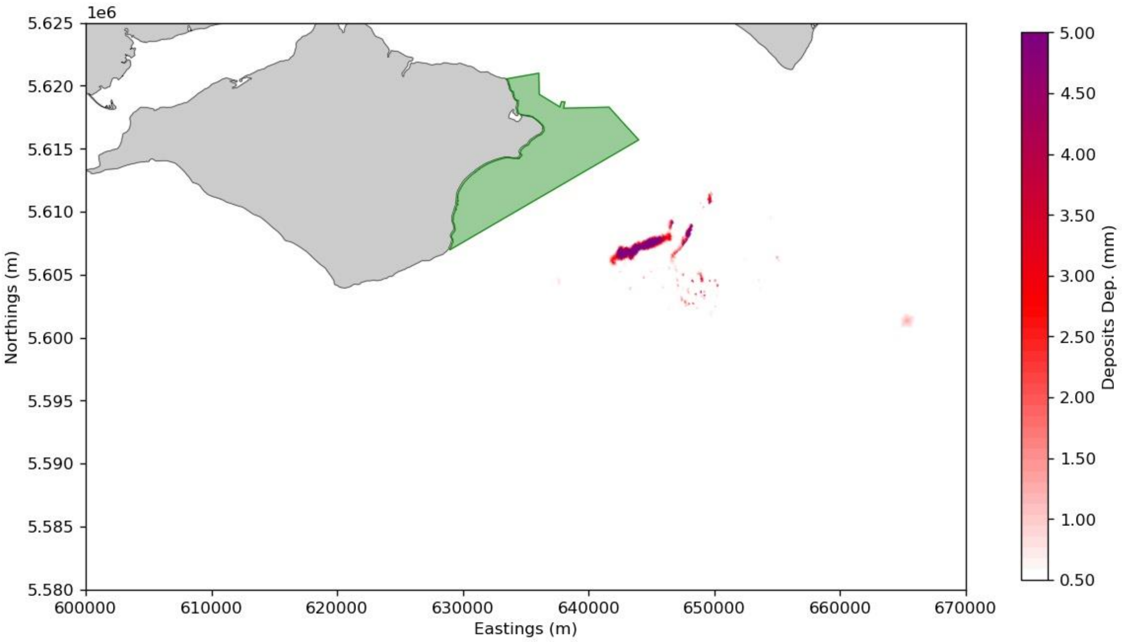

Figure 15 Footprint (based on an hourly sample rate) for non-cohesive fine (250 µm) sand, Scenario 8.

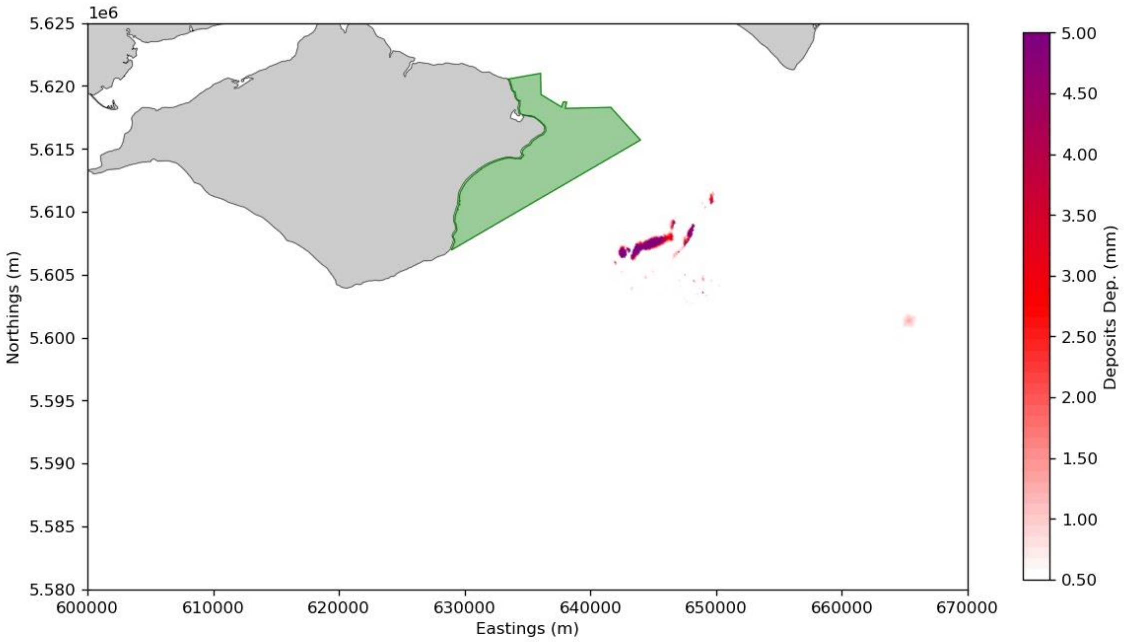

Figure 16 Snapshot of the deposits at the end of the 30-day simulation period for non-cohesive fine (250 µm) sand, Scenario 8.

5.4. Disposal of medium (500 µm) sand

The final sand fraction considered is medium sand comprising a mean grain diameter of 500 µm. This sand fraction has a higher fall velocity and requires a higher critical shear stress to be re-mobilised (eroded). As expected, it can be seen from the hourly footprint (Figure 17) that the deposits of medium sand remain localised to the disposal site. This is further evidenced when observing the sediment deposition at the end of the 30-day simulation (Figure 18): the sediments more-or-less remain in the locale of the disposal site, i.e.., no resuspension is occurring. It is possible under extreme storms that these sediments would be remobilized, however, in this case much of the seabed would be remobilised and thus the disposal would be integrated into the background.

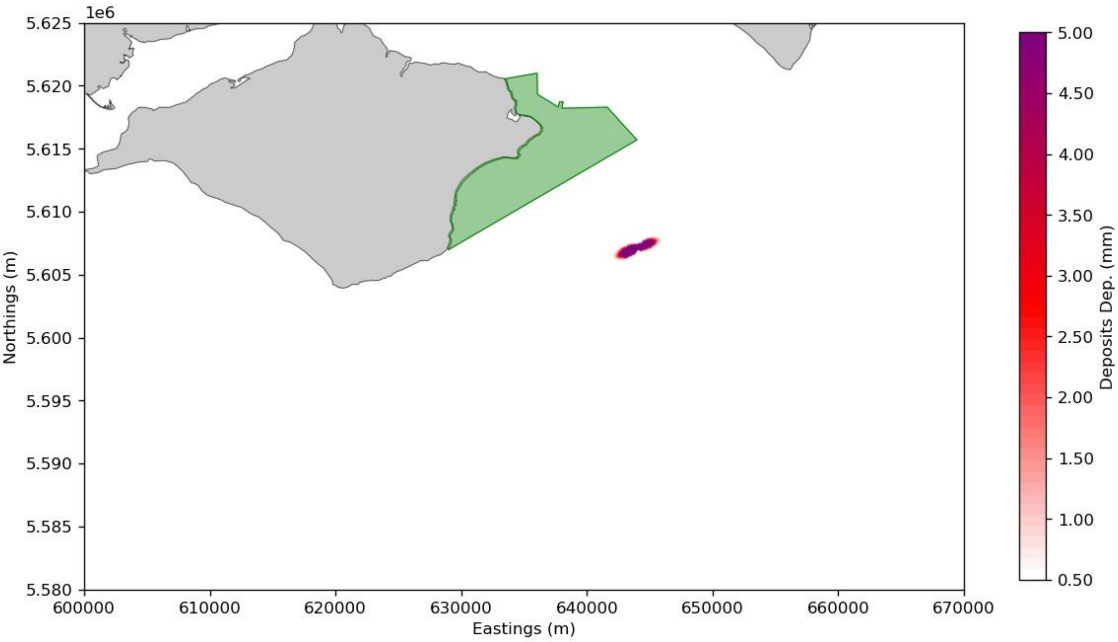

Figure 17 Footprint (based on an hourly sample rate) for non-cohesive medium (500 µm) sand Scenario 8.

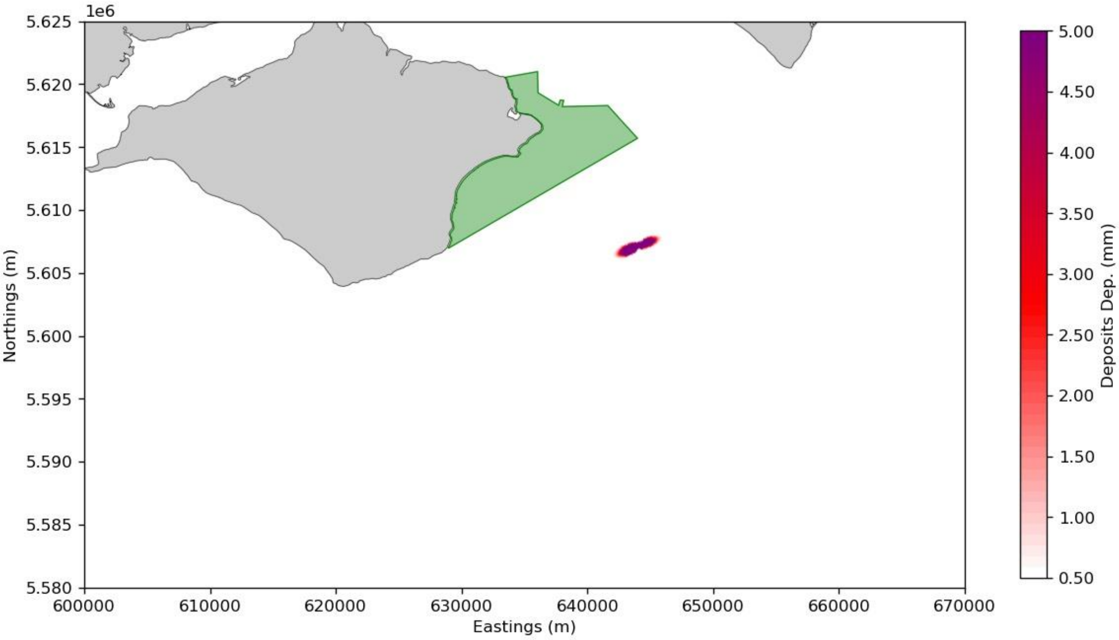

Figure 18 Snapshot of the deposits at the end of the 30-day simulation period for non-cohesive medium (500 µm) sand Scenario 8.

6. Conclusions

The model results clearly show that relatively course sediments (> 500 µm) disposed of at the NT disposal site remain in the immediate vicinity, potentially reaching sediment overburdens at the bed of up to 5 mm of thickness. The fine sand fraction of any material deposited at NT does get resuspended during a peak spring tide, but once deposited, remains in local depressions in the vicinity of the site or in the near vicinity to the east. Meanwhile, the very fine fraction of sand is initially deposited along the line of the tidal excursion, but the strong tides and residual current in the region result in a broad spread of this material, with some material being transported out of the domain. With respect to the fine (silt) fraction, there is some small immediate local deposition within the disposal site, but the strong tides in the region rapidly resuspend this material and redistribute it throughout the model domain at low concentrations.

In relation to the Bembridge MCZ, there does not appear to be either temporary or long-term deposition > 0.5 mm in the area.

Finally, due to the strong tides, the timing of disposal relative to the tidal frame (e.g. time before or after high water) has no effect on the eventual fate of the material or sediment overburden within the MCZ. Additionally, licence conditions imposing restrictions to certain wind directions would equally have little effect on sediment deposition within this tidally-driven system.

7. References

Astrium 2011. Creation of a high-resolution Digital Elevation Model (DEM) of the British Isles continental shelf: Final Report. Prepared for Defra, Contract Reference: 13820.

Battjes, J., and Janssen, J. 1978. “Energy loss and set-up due to breaking of random waves,.”In Proceedings 16th International Conference Coastal Engineering, ASCE, pages 569–587.44, 128, 133, 192.

Benson, T., Villaret, C., Kelly, D. M. and Baugh, J. 2014. Improvements in 3D sediment transport modelling with application to water quality issues. TELEMAC User Conference, Grenoble, France.

Bolam, S.G., Mason, C., Curtis, M., Griffith, A., Pettefor, A., Hawes, J., Fernand, L. and Beraud, C. 2018. Dredged Material Disposal Site Monitoring Round the Coast of England: Results of Sampling (2017-18), Cefas, Lowestoft.

Bolam, S.G., Barber, J., Curtis, M., Griffith, A., Hynes, C., Hawes, J., Mason, C., McIlwaine, P. and Warford, L. 2019. Dredged Material Disposal Site Monitoring Round the Coast of England: Results of Sampling (2018-19), Cefas, Lowestoft.

Cuthbertson A., Dong, P., King, S. and Davies, P., 2008. Hindered settling velocity of cohesive/non-cohesive sediment mixtures. Coastal Engineering 55 (2008) 1197–1208.

Flather, R.A., 1976. Results from a storm surge prediction model of the north-west European continental shelf 474 for April, November and December, 1973 Wormley, UK. Institute of Oceanographic Sciences 37pp.

Hasselmann, K., T. P. Barnett, E. Bouws, H. Carlson, D. E. Cartwright, K. Enke, J. Ewing, H. Gienapp, D. E. Hasselmann, P. Kruseman, A. Meerburg, P. Müller, D. J. Olbers,K. Richter, W. Sell and H. Walden, 1973. “Measurements of wind wave growth and swell decay during the Joint North Sea Wave Project (JONSWAP).” Deutsche Hydrographische Zeitschrift 8 (12).

Hervouet, J-M., 2007. Hydrodynamics of Free Surface Flows: Modelling with the Finite Element Method. Hydrodynamics of Free Surface Flows: Modelling with the finite element method. 10.1002/9780470319628.

Hill, A.,E., Brown, J., Fernand, L., Holt, J., Horsburgh, K.J., Proctor, R., Raine, R., Turrell, W.R., 2008. The thermohaline circulation of shallow tidal seas. Geophysical Research Letters 35 (11), art no L11605

Jacobs, W., Le Hir, P., van Kesterend, W. and Cann P., 2011. Erosion threshold of sand–mud mixtures. Continental Shelf Research, Vol. 31, Issue 10, Suppl. 1, pp S14-S25

Julien, P.Y., 2002, River mechanics: Cambridge, University Press, 434 p.

Komen, G., Hasselmann, S. and Hasselmann, K., 1984. On the existence of a fully developed wind-sea spectrum. Journal of Physical Oceanography 14: 1271–1285.

Manning, A.J., Baugh, J.V., Spearman, J.,R. and Whitehouse, R.J.S., 2010. Flocculation settling characteristics of mud: sand mixtures. Ocean Dynamics (2010) 60:237–253 DOI 10.1007/s10236-009-0251-0.

van der Molen, J., Ruardij, P., and Greenwood, N. 2015. Potential environmental impact of 18 tidal energy extraction in the Pentland Firth at large spatial scales: results of a 19 biogeochemical model. Biogeosciences Discussions, 12: 20475–20514.

Partheniades, E., 1965. Erosion and deposition of cohesive soils. Journal of the Hydraulics Division, ASCE, v. 91, No. HY1, Proceedings Paper 4204, p. 105–139.

Salehi, M., Kyle, S., 2012. Measurement of critical shear stress for mud mixtures in the San Jacinto estuary under different wave and current combinations. Continental Shelf Research.

Shi Benwei, Wang Ya Ping, Yang, Li Mingliang , Li Peng , Ni Wenfei and Gao Jianhua, 2015. Determination of critical shear stresses for erosion and deposition based on in situ measurements of currents and waves over an intertidal mudflat. Journal of Coastal Research.

Smolders, S., Bi, Q., Maximova, T. and Vanlede, J. 2018. Modelling Cohesive Sediments in the Scheldt Estuary (Belgium) with SEDI-3D. In: Bacon, John; Dye, Stephen; Beraud, Claire (Hg.): Proceedings of the XXVth TELEMAC-MASCARET User Conference, 9th to 11th October 2018, Norwich. Norwich: Centre for Environment, Fisheries and Aquaculture Science. S. 53-60.

Thorn, M.F.C., 1975. Loading and consolidation of dredged silt in a trailer suction hopper dredger in First International Symposium on Dredging Technology, A Symposium sponsored and organised by BHRA Fluid Engineering.

van Rijn, L.C, 1993. Principles of Sediment Transport in Rivers, Estuaries and Coastal Seas. Aqua Publications, The Netherlands. 82, 86, 338, 339, 340, 341, 342, 347, 351, 354, 355, 356, 556, 557.

van Rijn, L.C., 2007. United view of sediment transport by currents and waves I: Initiation of motion, Bed roughness and Bed load transport. Journal of Hydraulic Engineering, ASCE, Vol. 133, No. 6, p. 649-667.

Talbot, J.W. and Talbot, G.A., 1974. Diffusion in shallow seas and in English coastal an estuarine waters, in Physical Processes responsible for dispersal of pollutants in the sea. ICES Rapport et poces-verbaux des reunions vol 1967.

Tsanis I.,K., 1988 Simulation of wind-induced water currents, Journal of Hydraulic Engineering 115 (8), 1113-1134.

Uncles, R.J., Stephens, J.A. and Harris, C., 2015. Physical processes in a coupled bay-estuary coastal system: Whitsand Bay and Plymouth Sound. Progress in Oceanography 137 (2015) pp. 360-384.

Winterwerp J.C., van Kesteren W.G.M., van Prooijen B. and Jacobs W., 2012. A conceptual framework for shear flow–induced erosion of soft cohesive sediment beds. Journal of Geophysical research, vol. 117, C10020, doi:10.1029/2012JC008072.

Centre for Environment Fisheries & Aquaculture Science

Cefas

World Class Science for the Marine and Freshwater Environment

We are the government's marine and freshwater science experts. We help keep our seas, oceans and rivers healthy and productive and our seafood safe and sustainable by providing data and advice to the UK Government and our overseas partners. We are passionate about what we do because our work helps tackle the serious global problems of climate change, marine litter, over-fishing and pollution in support of the UK's commitments to a better future (for example the UN Sustainable Development Goals and Defra's 25 year Environment Plan).

We work in partnership with our colleagues in Defra and across UK government, and with international governments, business, maritime and fishing industry, non-governmental organisations, research institutes, universities, civil society and schools to collate and share knowledge. Together we can understand and value our seas to secure a sustainable blue future for us all, and help create a greater place for living.

Pakefield Road, Lowestoft, Suffolk, NR33 0HT

The Nothe, Barrack Road, Weymouth DT4 8UB

www.cefas.co.uk | +44 (0) 1502 562244